

Total Hadronic (π^- , Ar) Cross Section for Run-II

Authors: Jonathan Asaadi, Elena Gramellini

Abstract

Puppa

Contents

1	Tracking Studies	2
1.1	Angular Resolution	2
2	Energy Studies	2
2.1	dE/dX	2
2.2	Energy Deposited	3
3	Outline Of the Measurement	6
4	Background Subtraction	7
4.1	Beam Composition	7
4.1.1	Contamination from Beamline Electrons and Muons	7
4.1.2	Contamination from secondaries at TPC Front Face	8
4.2	Propagation and Filter	8
4.3	Background Contribution to the Cross Section	8
4.4	Systematics on Background Subtraction	10
5	Efficiency Correction	10
5.1	Systematics on Efficiency Correction	10

1 Tracking Studies

1.1 Angular Resolution

Scope of this study is to understand and compare the tracking performances and angular resolution of the TPC tracking on data and MC. We use the angular resolution of the tracking to determine the value of smallest angle that we can reconstruct with a non-zero efficiency, effectively determining a selection on the angular distribution of the cross section measurement due to the tracking performances.

We use the same procedure to evaluate the tracking performance in data and MC outlined in this section. We start by selecting all the WC2TPC matched tracks, that are the tracks used for the cross section analysis. These tracks can contain from a minimum of 3 3D-space points to a maximum of 240 3D-space points. We fit a line to all the 3D space points associated with the track. For each track we calculate the average distance between each 3D point in space and the fit line as follows

$$\bar{d} = \frac{\sum_i^N d_i}{N}, \quad (1)$$

where N is the number of point of the track and d_i is the distance of the i -th space point to the line fit. Several tests to compare the goodness of fit between data and MC have been considered. We decided to use \bar{d} for its straightforward interpretation. The \bar{d} distribution for data and MC is shown in Figure ??.

A visual representation of the procedure used to evaluate the angular resolution is shown in Figure 1. For each track, we order the space points according to their Z position (along the positive beam direction) and we split them in two sets: the first set contains all the points belonging to the first half of the track and the second set counts all the points contains to the second half of the track. We remove the last four points in the first set and the first four points in the second set, so to have a gap in the middle of the original track. We fit the first and the second set of points with a line separately. We then calculate the angle between the fit of the first and second half α . The angle α determines the spatial resolution of the tracking. The distributions for data and MC for α are given in 2. The mean of the data and MC angular resolution are respectively

$$\bar{\alpha}_{Data} = (4.7 \pm 3.3) \text{ deg} \quad (2)$$

$$\bar{\alpha}_{MC} = (4.5 \pm 3.2) \text{ deg}. \quad (3)$$

A small, 0.2 deg systematic shift between the mean of the data and MC angular resolution is present, which we account for in the context of the MC efficiency correction to the cross section, as presented in 5.1.

2 Energy Studies

A study we did was to look at the difference between DATA/MC in the dE/dX and energy deposited. We basically found there is very little difference between the two and we try to quantify how much the difference is.

2.1 dE/dX

Figure 3 shows the output of the fit of the Pion MC and the 60 Amp data. The MC is normalized to the data and both are fit to a Landau function. ^a

The difference between the two MPV's, is 2.4% between the data and the MC.

Figure 4 shows the stacked version of the dE/dX with the backgrounds stacked. The backgrounds are given in the ratio of 68.8% pion, 4.6% muon, and 26.6% electron. Once they are taken in these ratios, the sum of the MC is normalized to the sum of the data.

For completeness, the log scale versions of are shown in Figure 5.

Plotting scripts can be found here on [lariatgpvm](#)

`/lariat/app/users/jasaadi/v06_34_01_PionWeek/PlottingScripts`

and the samples were put here

`/lariat/data/users/elenag/theFinalPions/TPCDATA`

`/lariat/data/users/elenag/theFinalPions/TPC_MC/`

^aThe entries at dE/dX = 0 come from an uninitialized variable and can/should be taken out of these plots

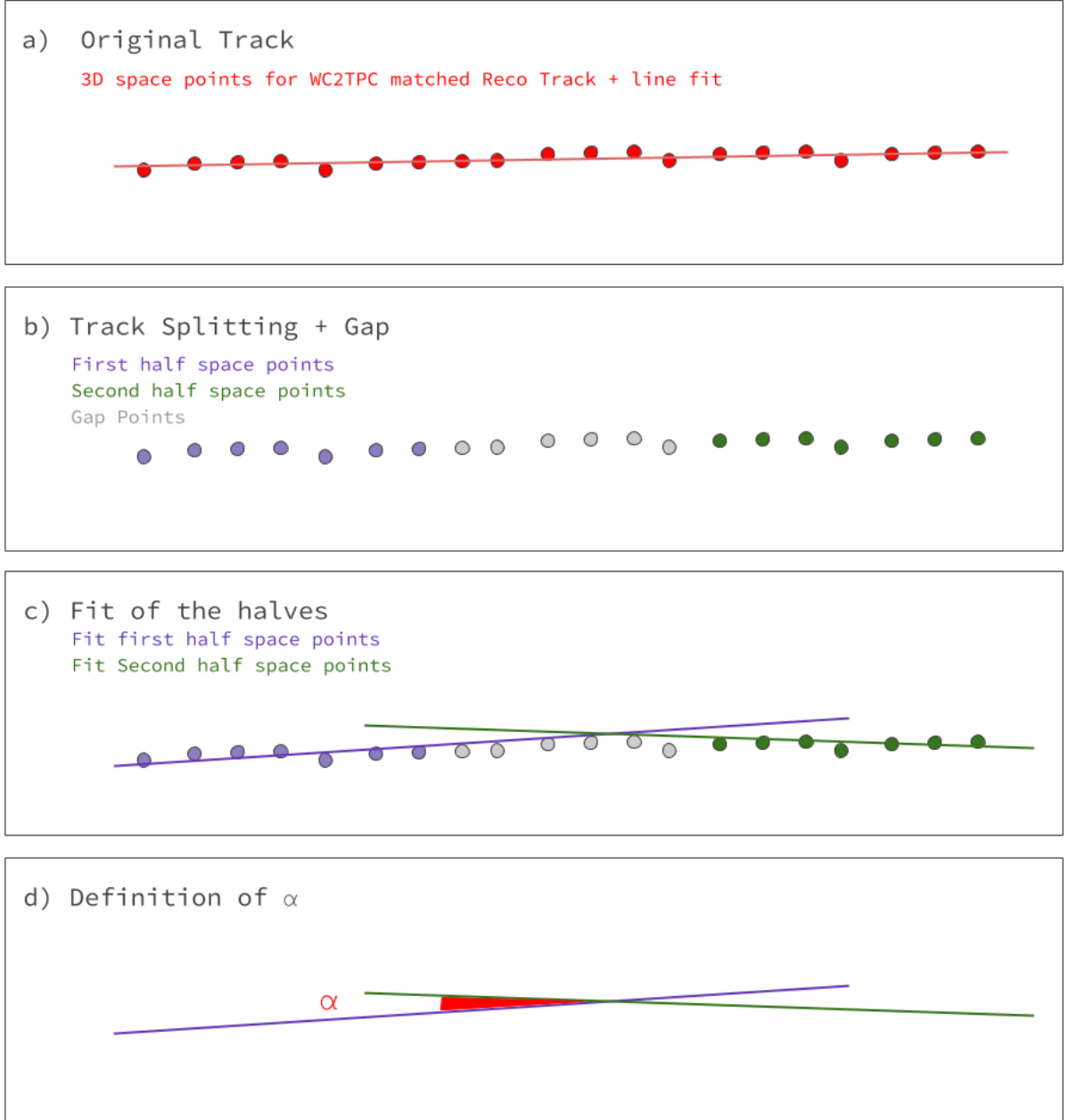


Figure 1: Sketch of the procedure used to determine the angular resolution.

2.2 Energy Deposited

The initial energy the particle has as it enters the TPC is given by

$$KE_{Initial} = \sqrt{P_{WCtrk}^2 + m_\pi^2} - m_\pi - E_{Loss} \quad (4)$$

and the uncertainty of the initial energy $\delta KE_{Initial}$ is given by

$$\delta KE_{Initial} = \sqrt{\delta P_{WCtrk}^2 + \delta E_{Loss}^2} \quad (5)$$

If we assume the uncertainty is 2% as the Minerva experiment had, and our uncertainty on the energy loss upstream is 7 MeV, then the total uncertainty on the initial kinetic energy for a typical 500 MeV pion is ~ 12 MeV.

Now the energy for j^{th} slab of the incident histogram is given by

$$KE_j^{Incident} = KE_{Initial} - \left(\sum_{i < j} dE/dX_i \times Pitch_i \right) \quad (6)$$

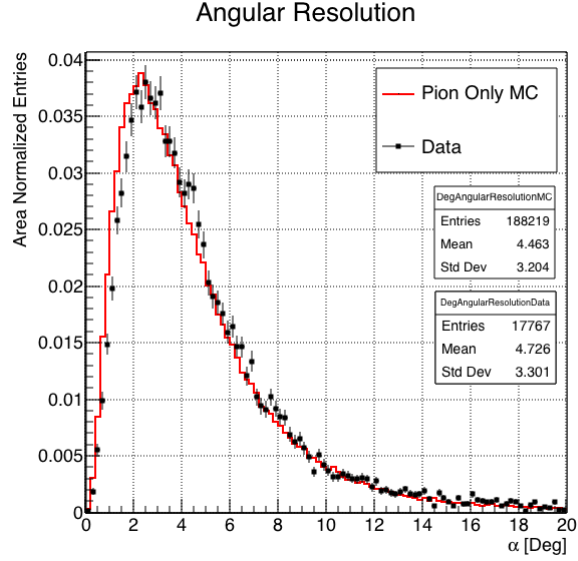


Figure 2: Distributions of angular resolution α for data used in the pion cross section analysis and pion only DDMC. The distributions are area normalized.

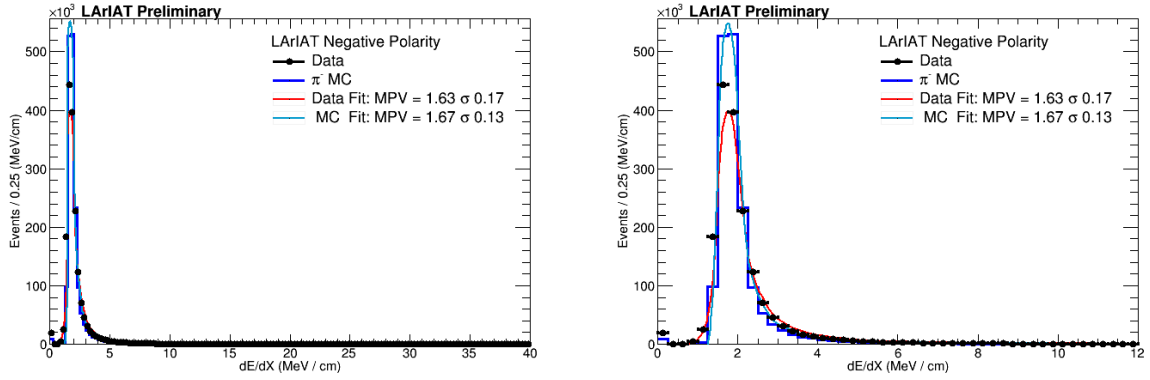


Figure 3: dE/dX for 60Amp data and data driven pion MC, both fit with a Landau

where i is given by the slab you are at, dE/dX_i is the energy deposited at that slab, and $Pitch_i$ is the pitch for that point.

Thus we can talk about the energy at the j^{th} slab as

$$E_j^{slab} = \left(\sum_{i < j} dE/dX_i \times Pitch_i \right) \quad (7)$$

The systematic uncertainty of E_j^{slab} is given by the difference between this quantity in data and MC, and the uncertainty on E_j^{slab} is given by the width of the Landau fit to the data. These are shown in Figure 6

The difference between the MPV of data and MC is 1.0% ($0.0784 - 0.0776 / 0.0784$) and thus the systematic uncertainty you would assign to the energy in the incident kinetic energy would be for all 240 slices (assuming you have 240 slices at 0.4 mm pitch) and thus is

$$\delta E_j^{slab} = (0.0784 - 0.0776) \times 240 = 0.008 MeV \times 240 = 1.92 MeV \quad (8)$$

So the uncertainty on the incident kinetic energy is given by

$$\delta KE^{Incident} = \sqrt{(\delta KE_{Initial})^2 + (\delta E_j^{slab})^2} = \sqrt{(12 MeV)^2 + (2 MeV)^2} = 12.1 MeV \quad (9)$$

Figure 7 shows the stacked version of the Energy Deposited plots with the backgrounds stacked. The backgrounds are given in the ratio of 68.8% pion, 4.6% muon, and 26.6% electron. Once they are taken in these ratios, the sum of the MC is normalized to the sum of the data.

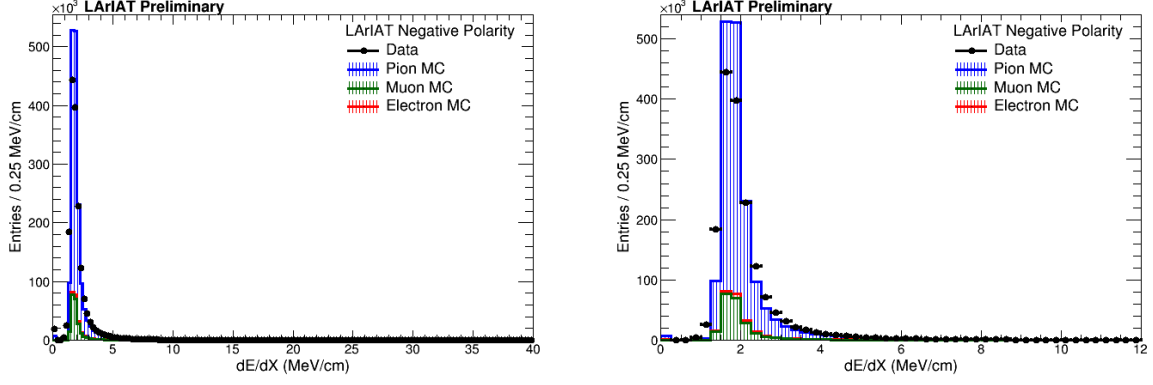


Figure 4: Stacked versions of the dE/dX with the data and electron/muon/pion MC.

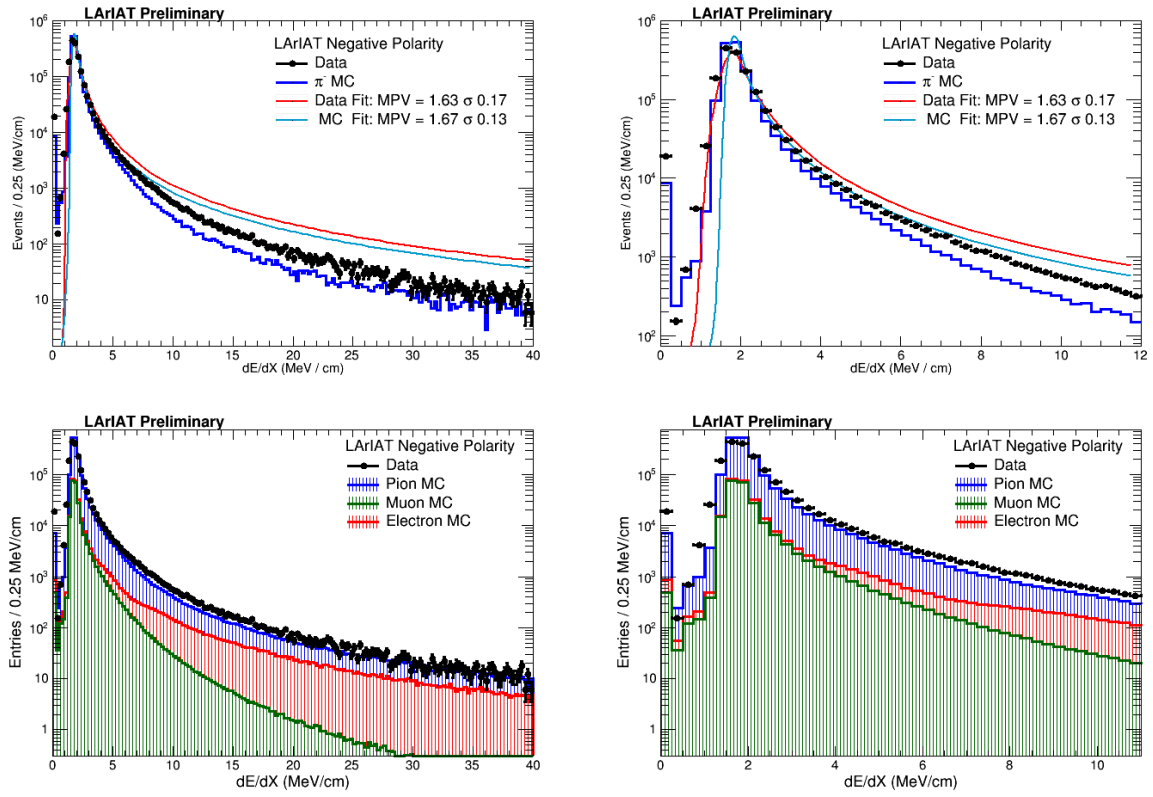


Figure 5: dE/dX for 60Amp data and MC shown in log scale

The energy at the interacting point is given by

$$KE_{Interaction} = \sqrt{P_{WCTrk}^2 + m_{\pi}^2} - E_{Loss} - (\Sigma dE/dX_i \times Pitch) \quad (10)$$

and has the exact same uncertainty as the incident kinetic energy plot. Thus these estimates can be applied to getting the uncertainty on the energy of the reconstructed cross-section.

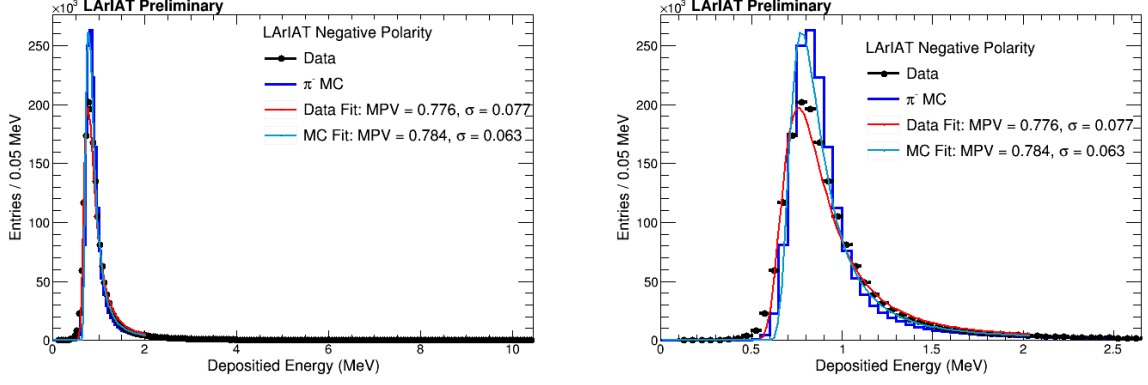


Figure 6: Energy Deposited in Pion MC and 60A data.

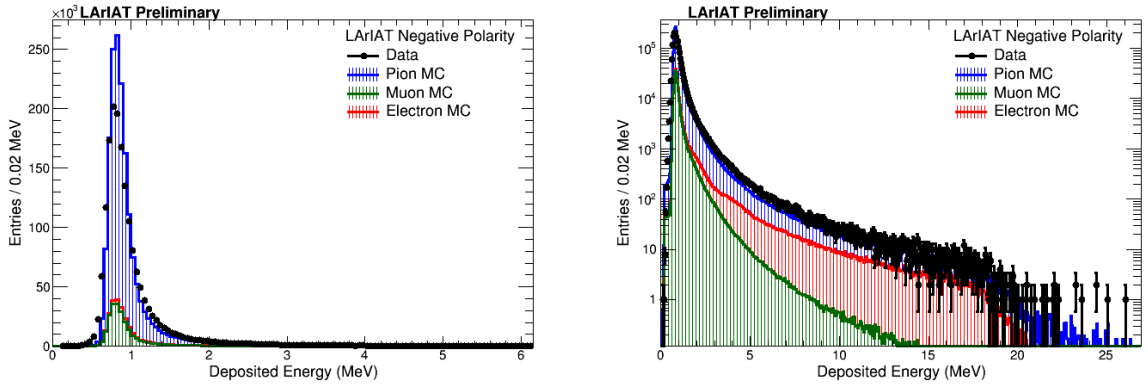


Figure 7: Energy Deposited with all the MC and 60A data.

3 Outline Of the Measurement

If LArIAT had a beam of pure pions and were 100% efficient in determining the interaction point within the TPC, the pion cross section in each energy bin would be given by

$$\sigma^{\pi^-}(E_i) = \frac{1}{n\delta X} \frac{N_{Interacting}^{\pi^-}(E_i)}{N_{Incident}^{\pi^-}(E_i)}. \quad (11)$$

Unfortunately, this is not the case. The selection used to isolate pions in the LArIAT beam allows for the presence of some muons and electrons as contaminants. Also, the LArIAT TPC is not 100% efficient in determining the interaction point. Therefore we need to apply two corrections in order to extract the true pion cross section from LArIAT data: the background subtraction and the efficiency correction. We estimate the true pion cross section in each energy bin changing the equation 11 into

$$\sigma^{\pi^-}(E_i) = \frac{1}{n\delta X} \frac{N_{Interacting}^{\pi^-}(E_i)}{N_{Incident}^{\pi^-}(E_i)} = \frac{1}{n\delta X} \frac{\epsilon_i^{inc}[N_{Interacting}^{TOT}(E_i) - B_{interacting}(E_i)]}{\epsilon_i^{int}[N_{Incident}^{TOT}(E_i) - B_{incident}(E_i)]}, \quad (12)$$

where $N_{Interacting}^{TOT}(E_i)$ and $N_{Incident}^{TOT}(E_i)$ is the measured content of the data interacting and incident histograms respectively, $B_{interacting}(E_i)$ and $B_{incident}(E_i)$ represent the contributions from beamline contaminants, and ϵ_i^{int} and ϵ_i^{inc} are the efficiency corrections for said histograms.

As we will show in section 4.3, the background subtraction for the interacting and incident histograms can be translated into the corresponding corrections $C_{Interacting}^{\pi MC}(E_i)$ and $C_{Incident}^{\pi MC}(E_i)$ and the cross section re-written as follows

$$\sigma^{\pi^-}(E_i) = \frac{1}{n\delta X} \frac{\epsilon_i^{inc} N_{Interacting}^{TOT}(E_i) C_{Interacting}^{\pi MC}(E_i)}{\epsilon_i^{int} N_{Incident}^{TOT}(E_i) C_{Incident}^{\pi MC}(E_i)}. \quad (13)$$

The following sections describe the procedures used to evaluate the background subtraction (section 4) and the efficiency correction (section 5) and the estimate of their uncertainties. The reader might be concerned about bin-by-bin migration of events in the interacting and incident plots due to the finite resolution

of the energy reconstruction. In section 2.2, we make an argument to why we expect the smearing matrix to be extremely close to diagonal and its calculation is left for an improvement of the current analysis.

4 Background Subtraction

Even if pions are by far the biggest component of the beam in negative polarity runs, the LArIAT beam is not a pure pion beam. While useful to discriminate between pions/muons/electrons, kaons, and protons, the beamline detectors are not sensitive enough to discriminate among the lighter particles in the beam: electrons, muons and pions fall under the same mass hypothesis. Thus, we need to assess the contamination from beamline particles other than pions in the event selections used for the pion cross section analysis and correct for its effects.

4.1 Beam Composition

We define beamline contamination every TPC track matched to the WC track which is not a primary pion. Potentially, there are 4 different types of beamline contaminations:

- 1) electrons,
- 2) muons,
- 3) secondaries from pion events,
- 4) matched pile up events.

The first step is to estimate what percentage of events used in the cross section calculation is not a primary pion. The next two sections will illustrate this estimate for the electrons, muons and secondaries from pion event. We estimate the last type of contamination, the “matched pile up” events, to be a negligible fraction, because of the definition of the WC2TPC match: we deem the probability of a single match with a halo particle in the absence of a beamline particle^b negligibly small. **SHOW VTX distribution in WC2TPC match**

4.1.1 Contamination from Beamline Electrons and Muons

We estimate the percentage of electrons and muons in the beam via the G4Beamline MC. Since the beamline composition is a function of the magnet settings, we simulate separately events for magnet current of -60A

^b Events with multiple WC2TPC matches are always rejected.

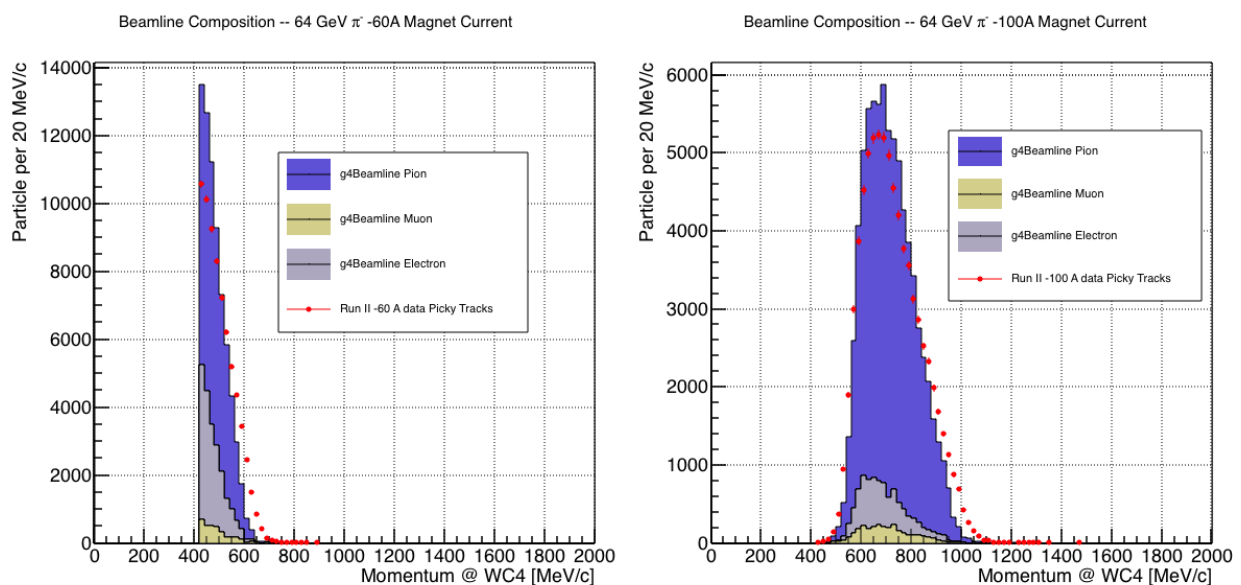


Figure 8: Beam composition for the -60A runs (left) and -100A runs (right). The solid blue plot represents the simulated pion content, the yellow plot represents the simulated muon content and the grey plot represents the simulated electron content. The plots are area normalized to the number of data events, shown in red.

and -100A. Table 1 shows the beam composition per magnet setting after the mass selection according to the G4Beamline simulation.

Figure 8 shows the momentum predictions from G4Beamline overlaid with data for the 60A runs (left) and for the 100A runs (right). The predictions for electrons, muons and pions have been staggered and their sum is area normalized to data, which is shown in red. Albeit not perfect, these plots show a reasonable agreement between the momentum shapes in data and MC. We attribute the difference in shape to the lack of simulation of the WC efficiency in the MC which is momentum dependent and leads to enhance the number events in the center of the momentum distribution.

Once the beam composition at WC4 is known, we simulate the electrons, muons and pions with the DDMC and we subject the three samples to the same selection chain (WC2TPC match, shower filter, pile up filter). The percentage of electrons and muons surviving the selection chain weighted by the beam composition is the electron and muon contamination in the pion cross section sample, as shown in Table 2.

4.1.2 Contamination from secondaries at TPC Front Face

Pions can travel the length of the LArIAT beamline and interact hadronically in the steel or in the non-instrumented argon upstream to the TPC front face. Or, they could decay in flight between WC4 and the TPC. One of the interaction products can leak into the TPC and be matched with the WC track, contributing to the pool of events used for the cross section calculation. We call this type of particles “secondaries” from pion events, with a terminology inspired by Geant4. We estimate the number of secondaries using the DDMC pion sample. The percentage of secondaries is given by the number of matched WC2TPC tracks whose corresponding particle is not flagged as primary by Geant4. The secondary to pion ratio is $X\%$ in the 60A sample and $Y\%$ in the 100A sample.

4.2 Propagation and Filter

Once we have estimated the beam composition at WC4, the next step is propagating pions, muons and electrons into the TPC and evaluate their collective contribution to the cross section. To do so, we simulate the same number of electrons, muons and pions with the DDMC and we apply the same selection filters on the three samples. The number of events per particle species surviving this selection is shown on table 2.

4.3 Background Contribution to the Cross Section

We then produce the interacting and incident histograms for the events surviving the selection for both the pions and the contaminants, weighted by the estimated beam composition. From the histograms in Figure 9, we are able to evaluate the relative contribution of the contaminants to each bin of the interacting and incident histograms separately and obtain the respective corrections for data. We take here the interacting histogram as example, noting that the derivation is identical for the incident histogram. The number of entries in each bin of the interacting plot (Figure 9 left) is $N_{Interacting}^{TOT}(E_i)$, equal to the sum of the pions and contaminants in that bin, namely

$$N_{Interacting}^{TOT}(E_i) = N_{Interacting}^{\pi}(E_i) + \underbrace{N_{Interacting}^{\mu}(E_i) + N_{Interacting}^e(E_i) + N_{Interacting}^{Secondary}(E_i)}_{B_{Interacting}(E_i)}. \quad (14)$$

Thus, the relative contribution of pions to each bin in MC can be calculated as follows

$$C_{Interacting}^{\pi MC}(E_i) = \frac{N_{Interacting}^{\pi MC}(E_i)}{N_{Interacting}^{TOT MC}(E_i)} = \frac{N_{Interacting}^{TOT MC}(E_i) - B_{Interacting}^{MC}(E_i)}{N_{Interacting}^{TOT MC}(E_i)}. \quad (15)$$

In order to evaluate the pion content of each bean in data, we multiply the measured content of each bin by the corresponding relative pion contribution found in MC, as follows

$$N_{Interacting}^{\pi Data}(E_i) = N_{Interacting}^{TOT Data}(E_i) - B_{Interacting}^{Data}(E_i) = C_{Interacting}^{\pi MC}(E_i) N_{Interacting}^{TOT Data}(E_i). \quad (16)$$

We estimate the systematic uncertainty on the cross section from this subtraction procedure by varying the electron to pion and muon to pion ratio in a suitable range of values. Figure

	I = -60 A	I = -100 A
G4Pions	68.8 %	87.4 %
G4Muons	4.6 %	3.7 %
G4Electrons	26.6 %	8.9 %

Table 1: Simulated beamline composition per magnet settings

	π^- 60A	μ^- 60A	e^- 60A	π^- 100A	μ^- 100A	e^- 100A
Total Initial events	334500	334500	334500			
After Multiplicity Rejection	331313	322436	186261			
After WC2TPC: Selection	201458	285686	79109			
Evts After Shower Rejection	191655	277914	17477			
Selection Survival Rate	57%	83%	5%			
Beam Composition @WC4	68.8%	4.6 %	26.6 %	87.4 %	3.7 %	8.9 %
Beam Composition @TPC FF						

Table 2: MC selection flow per particle species.

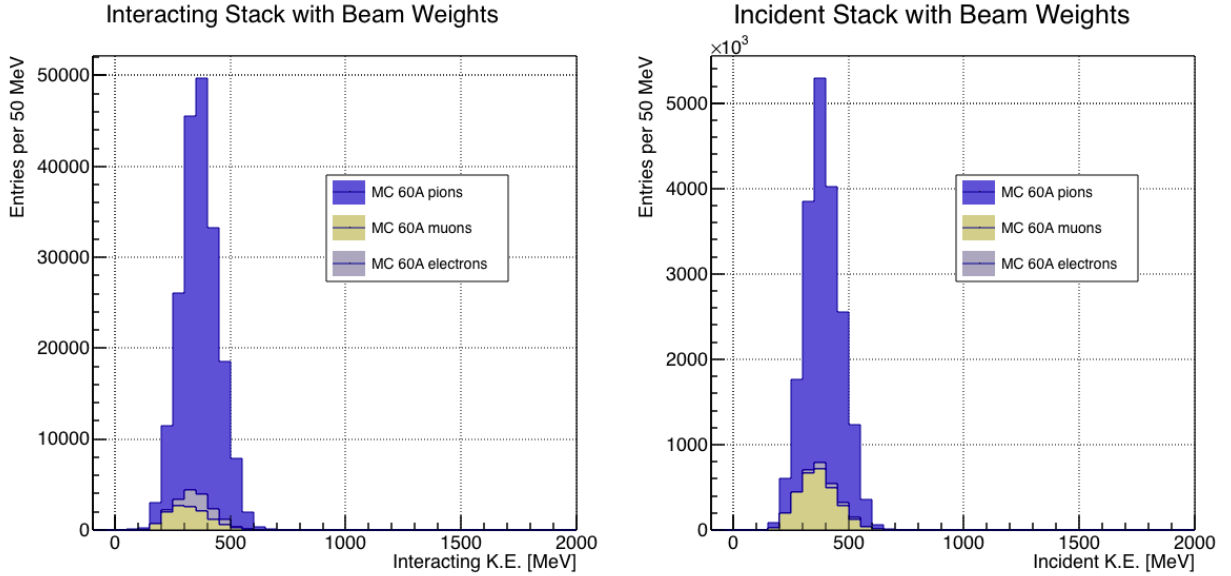


Figure 9: Left: staggered contributions to the interacting kinetic energy distribution for electron (grey), muons (yellow) and pion (blue) in the 60A simulation sample. Right: staggered contributions to the incident kinetic energy distribution for electron (grey), muons (yellow) and pion (blue) in the 60A simulation sample.

4.4 Systematics on Background Subtraction

5 Efficiency Correction

5.1 Systematics on Efficiency Correction